1 Introduction

1.1 The Integer Quantum Hall Effect

In 1980 – about a century after the discovery of the classical Hall effect by Edwin Hall in 1879 [1] – K. von Klitzing, G. Dorda, and M. Pepper announced the discovery of surprising transport properties of a two-dimensional electron gas in a Si metal-oxide field effect transistor (MOSFET) [2]. In these systems, the electrons are confined to a narrow layer near the metal-oxide interface such that they only populate the lowest quantum state perpendicular to the interface and effectively move only within the plane parallel to the interface.

Von Klitzing and co-workers measured both longitudinal and Hall (transverse) resistance as a function of carrier density n in strong magnetic fields B and at low temperatures T. Their original data is shown in Fig. 1.1. Remarkably, the Hall resistance exhibited plateau regions as a function of carrier density where it assumed values very close to h/je^2. Here, h denotes Planck's constant, e is the electron charge, and $j = 1, 2, \ldots$ an integer number. The precision of this quantization of the Hall resistance improves with decreasing temperature. Whenever the Hall resistance exhibits a plateau, the longitudinal resistance was found to drop to near zero with activated temperature dependence. This behavior was in stark contrast to the predictions of a simple Drude model [3] where, in the strong-field limit $\omega_c\tau \gg 1$, the Hall resistivity $\rho_H = B/en$ and the longitudinal resistivity $\rho_L = m^*/e^2n\tau$ depend smoothly on the carrier density n ($\omega_c = eB/m^*$ is the cyclotron frequency, m^* the effective mass of the electrons, and τ the carrier mean free path). In the meantime, the extraordinary precision of the quantization of the Hall resistance is exploited for the definition of a resistance standard [4].

Soon after the experimental discovery, this *integer quantum Hall effect* (IQHE) was understood as a consequence of the Landau quantization of the electronic eigenstates in high magnetic fields combined with electron localization by disorder. It is generally believed that in non-quantizing magnetic fields, all electronic eigenstates of two-dimensional systems are Anderson localized irrespective of the strength of the disorder potential [5]. By contrast, in quantizing magnetic fields one finds that the eigenstates remain extended at one energy within the Landau level with all other eigenstates being localized. This behavior is sketched in Fig. 1.2. Plateaus of the Hall resistance and zeros of the longitudinal resistance are observed whenever the chemical potential resides in the region of localized states. Transitions between plateaus occur when the chemical potential crosses the energy of the extended state. Relying on gauge invariance, Laughlin [7] gave a very general argument for the integer quantization of the Hall resistance when the chemical potential lies in a mobility gap. A sketch of

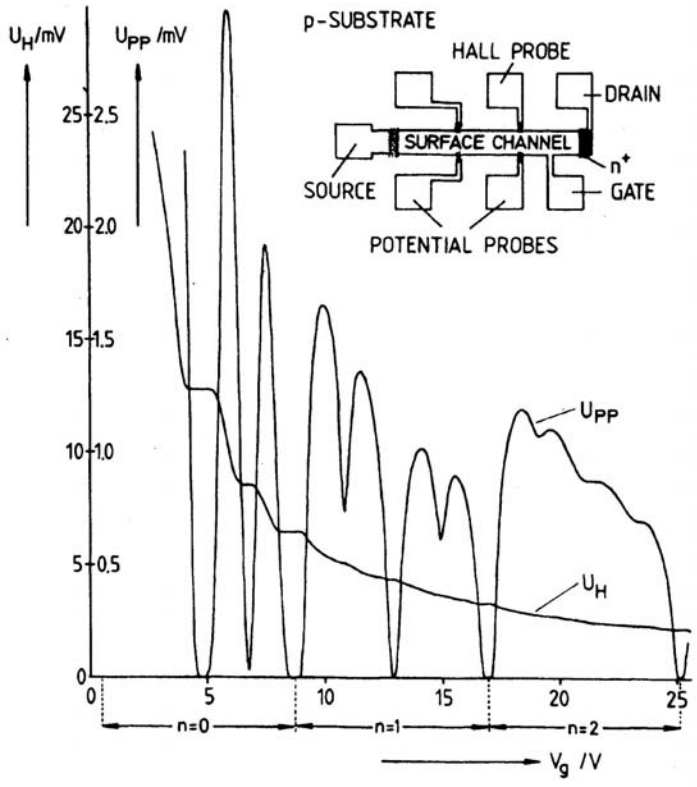

Figure 1.1: Experimental results for the Hall voltage U_H and the longitudinal voltage U_{PP} at $T = 1.5$ K and $B = 18$ T as a function of the gate voltage V_g which is directly related to the carrier density n. The inset shows a top view of the device with dimensions 400×50 μm. This figure has been taken from Ref. [2].

Laughlin's gedankenexperiment is given in Fig. 1.3.[1]

1.2 The Fractional Quantum Hall Effect

A couple of years after the discovery of the IQHE, D. C. Tsui, H. L. Stormer, and A. C. Gossard [9] discovered quantization of the Hall resistance at fractional values of j, namely $j = 1/3$ and $2/3$. These experiments were performed on two-dimensional electron systems at the interface of GaAs/AlGaAs heterostructures at even lower temperatures and higher magnetic fields. These systems allow for higher electron mobilities due to modulation doping which removes the defects from the plane of the two-dimensional electron system. Unlike the IQHE, which occurs whenever the electrons approximately fill an integer number of Landau levels (LL), this *fractional quantum Hall effect* (FQHE) is observed when all electrons are in the lowest Landau level (LLL) and 1/3 or 2/3 of all states of

[1] A particularly lucid version of this argument was later given by Halperin [8].

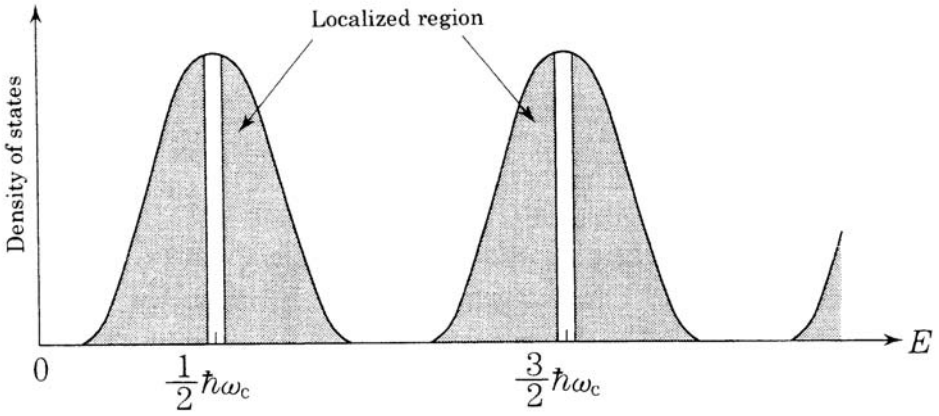

Figure 1.2: Sketch of the density of states of a 2DEG in a perpendicular magnetic field showing regions of extended states (in white) near the center of the impurity-broadened Landau levels, i.e. at $E \simeq (n + 1/2)\hbar\omega_c$, and regions of localized states (in gray). This figure has been taken from Ref. [6].

the Landau level are occupied (Landau level filling factor[2] 1/3 and 2/3).

Despite the great similarities in the phenomenology of the integer and fractional effects, there are significant differences in their theoretical explanations. When all electrons are residing in the lowest Landau level, their kinetic energy is effectively frozen out by the Landau quantization and the dominant term in the Hamiltonian is given by the Coulomb interaction between the electrons. If the electrons could be treated as classical, this would imply a Wigner-crystal ground state, in which the electrons order in a triangular lattice. However, due to the magnetic field, the X- and Y-coordinates of the guiding centers (i.e., the centers of the cyclotron orbits) are canonically conjugate variables with a nonvanishing commutator. This implies, via the uncertainty relation, that the guiding centers are no longer sharply defined and quantum fluctuations effectively grow with increasing electron density. Laughlin argued that these quantum fluctuations melt the Wigner crystal in the range of filling factors where the fractional quantum Hall effect occurs, resulting in a correlated electron liquid (Laughlin states). He further argued, by constructing explicit many-body trial wavefunctions, that this correlated electron liquid becomes incompressible at filling factors equal to $\nu = 1/q$ with $q = 3, 5, \ldots$ an odd integer. These states are characterized by a finite energy gap for the creation of quasiparticle (and quasihole) excitations. Roughly, it is this energy gap which is analogous to the cyclotron gap for completely filled Landau levels in the integer quantum Hall effect.

Laughlin derived his trial wavefunction for the many-particle state by the following reasoning [11]. For high magnetic fields, the single-electron eigenstates

[2]Each Landau level is macroscopically degenerate with a degeneracy D equal to the number of flux quanta through the sample, i.e., $D = BA/\phi_0$. Here, B denotes the magnetic field, A the area of the sample, and $\phi_0 = h/e$ the flux quantum. The Landau level filling factor ν is a measure of the number of filled Landau levels, $\nu = N/D = n\phi_0/B$, where N denotes the number of electrons and $n = N/A$ the electron density.

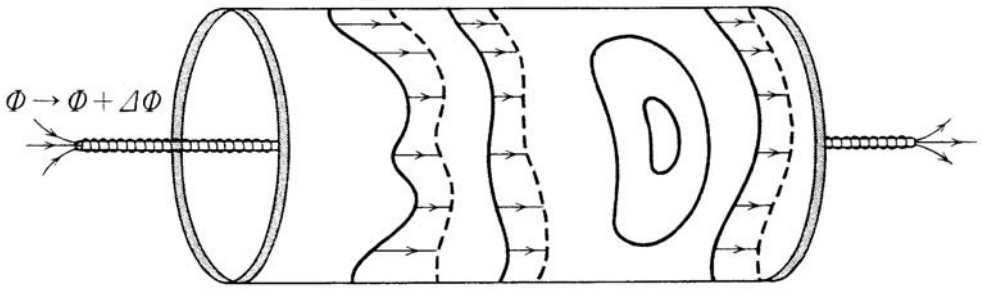

Figure 1.3: Simple picture of Laughlin's gauge argument in terms of transport of extended wavefunctions along a cylinder as the flux through an embedded solenoid is changed. Shown is a 2DEG bent on a cylindrical surface of radius R. The magnetic field is assumed to be perpendicular to the surface of this cylinder and constant. An additional solenoid is placed on the axis of the cylinder, generating a magnetic flux Φ through the cylinder, parallel to its axis. Within this gedankenexperiment, Laughlin was able to demonstrate that a change in the magnetic flux $\Phi \rightarrow \Phi + \Delta\Phi$ has a different effect on localized and extended states of electrons on the cylinder. Extended states – which surround the cylinder laterally in y-direction – must satisfy a periodicity condition of the form $\Psi(x, y + 2\pi R) = \Psi(x, y)$, while localized states – which are not connected in y-direction – do not have to fulfill such a condition. The gauge argument then shows that the change in flux $\Delta\Phi$ must satisfy $\Delta\Phi = h/e \times$ (integer) for extended states. The effect of a change in flux is then equivalent to a translation in x-direction for the extended states, while for the localized states, the effect is a mere change in phase. The extended states can thus carry a current through the system when a potential bias is applied at the ends of the cylinder. When all extended states below the Fermi level are occupied, this current does not change until the Fermi level crosses the next-higher lying extended state (typically lying at the center of the next-higher LL). Thus, the conductivity is quantized and of exactly that form observed in the QHE. This figure has been taken from Ref. [6].

are restricted to the lowest Landau level (LLL) $N = 0$ and, within the symmetric gauge, the states $|N = 0, m\rangle$ can be distinguished by their eigenvalue m with respect to the z-component L_z of angular momentum. The single-electron wavefunctions in position space are then given by

$$\varphi_{0,m}(z) = \frac{1}{\sqrt{2\pi 2^m m!}\ell_B} z^m e^{-|z|^2/4\ell_B^2} \quad , \tag{1.1}$$

where

$$z = (x - iy)/\ell_B$$

denotes the position of the 2D electron as a complex number and $\ell_B = \sqrt{\hbar/eB}$ is the magnetic length. This wavefunction represents an electron localized circularly as shown in Fig. 1.5.

In view of the single-electron wavefunctions, Eq. (1.1), any many-electron wavefunction must assume the form

$$\Psi(\mathbf{r}_1, \mathbf{r}_2, \ldots, \mathbf{r}_N) = p(z_1, ..., z_N) e^{-\sum_i |z_i|^2/4\ell_B^2} \tag{1.2}$$

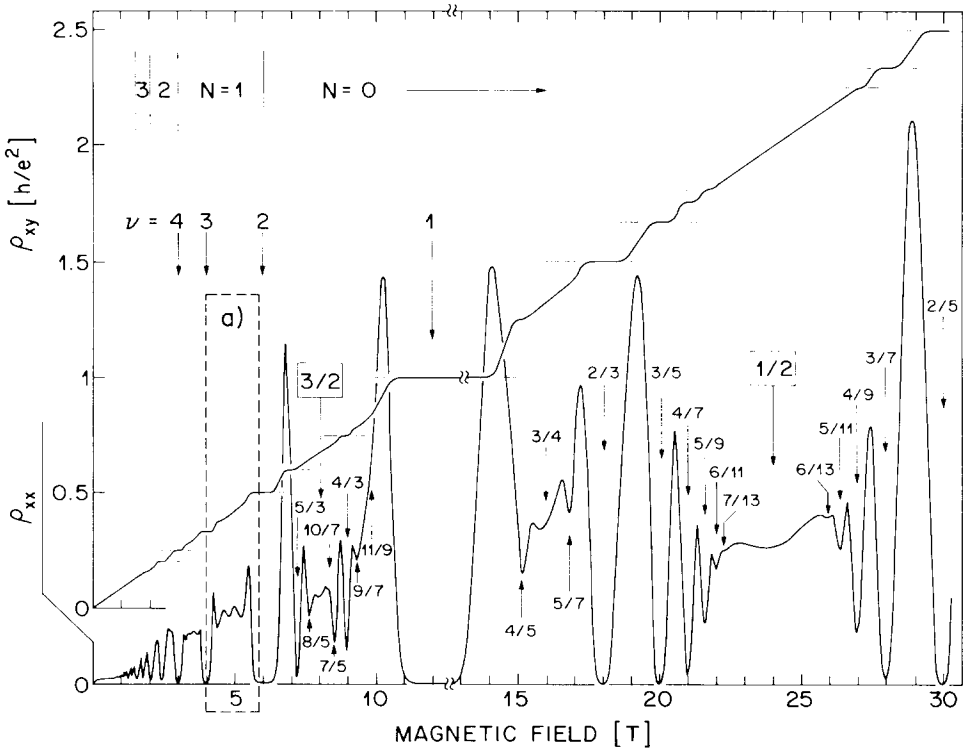

Figure 1.4: Experimental results by Willett and co-workers. Plotted are the Hall resistivity ρ_{xy} and the longitudinal resistivity ρ_{xx} of a 2D electron sample of electronic density $n = 3 \times 10^{11}$ cm^{-2} and mobility 1.3×10^6 cm^2/Vs at a temperature $T = 150$ mK versus magnetic field. The numbered arrows identify the filling factor ν which indicates the degree to which the Landau levels (labeled by N) are filled with electrons. In contrast to the expected linear behavior of $R_{xy}(B)$, the Hall resistance exhibits plateaus at quantized values of the resistance, $R_{xy} = h/(\nu e^2)$ coinciding with minima of R_{xx}. The figure is composed of four different traces, joined at a magnetic field ~ 12.5 T. The high-field values of the resistance are scaled down by a factor of 2.5 and, for a technical reason, have been measured at a temperature $T = 85$ mK. This figure has been taken from Ref. [10].

where $p(z_1, ..., z_N)$ is a polynomial in $z_1, ..., z_N$ which is antisymmetric under particle interchange. Laughlin showed that the Jastrow-type wavefunctions

$$\Psi_{gs}(z_1, ..., z_N) = \prod_{i<j} (z_i - z_j)^q e^{-\sum_i |z_i|^2/4\ell_B^2} \tag{1.3}$$

have large overlaps with numerically exact ground-state wavefunctions[3] at filling factors $1/q$. Due to the antisymmetry requirement, these Laughlin states are restricted to odd-denominator filling fractions. Laughlin also argued that the

[3]Haldane formulated a short-range interaction model for which the Laughlin wavefunction can be proven to be the exact and unique ground state [12].

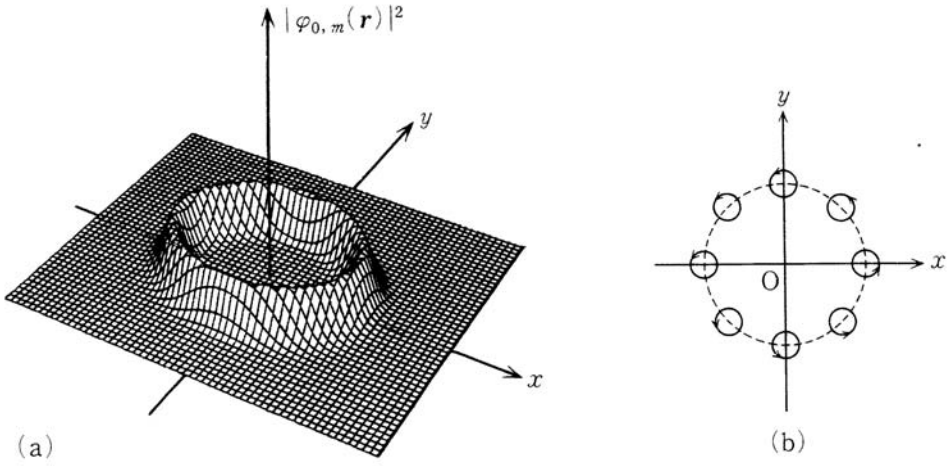

Figure 1.5: Lowest Landau level single electron wavefunction (a) and classical orbit corresponding to this wavefunction (b). The maximum of the existence probability $|\varphi_{0,m}(z)|^2$ lies on a circle of radius $\sqrt{2m}\ell_B$ and the spread towards each side of the circle is of the order of ℓ_B. The circle must not be identified with the classical cyclotron motion orbit, since the radius of the classical cyclotron motion is ℓ_B. As shown in (b), the state $|0,m\rangle$ can be interpreted as a classical superposition of many cyclotron orbits with radius ℓ_B and centers on a circle of radius $\sqrt{2m}\ell_B$. This figure has been taken from Ref. [6].

wavefunction

$$\Psi_{z_0}(z_1, z_2, ..., z_N) = \prod_{i=1}^{N}(z_i - z_0)\Psi_{gs}(z_1, z_2, ..., z_N) \tag{1.4}$$

describes a localized (hole) excitation, located at z_0. These quasiholes as well as similar quasiparticle excitations are indeed gapped and the system is incompressible.

The quasiparticles of fractional quantum Hall states carry fractional charge and obey fractional quantum statistics. A heuristic way of understanding the fractional charge of the quasiparticles exploits gauge invariance via the Byers-Yang theorem (all spectral properties of multiply-connected electronic systems are periodic in the magnetic flux threading the system, with the period given by the flux quantum ϕ_0) [13, 7]. We imagine that we introduce an infinitesimal hole into the two-dimensional electron system, pierced by a solenoid threaded by magnetic flux which slowly increases from zero to one flux quantum. Due to the energy gap, the adiabatic theorem guarantees that the final state is an eigenstate of the system. On the other hand, the time-varying flux induces a circular electric field which in turn, by virtue of the Hall conductance, drives a current away from (or towards) the flux line. In view of the quantized value of the Hall conductance, it is then easy to compute the charge effectively removed from (or accumulated near) the flux line in the process, which turns out to equal $e^* = e/m$ for the Laughlin states at filling factor $\nu = 1/m$. Due to the magnetic flux, these quasiparticles are vortex-like and following Arovas, Schrieffer, and Wilczek [14], the fractional statistics of quasiparticles can be

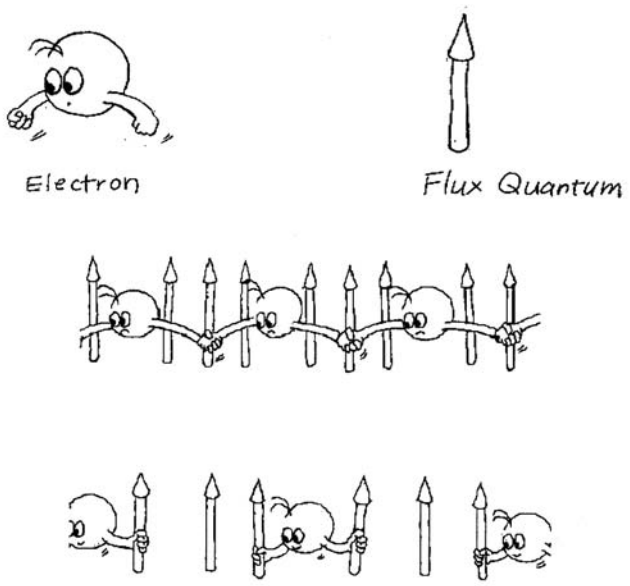

Figure 1.6: Kwon Park's humorous view of composite fermions. Strongly interacting electrons in a strong magnetic field (middle) can be mapped to weakly interacting electrons in a reduced effective magnetic field (bottom) by picking up two flux quanta each. This figure has been taken from Ref. [15].

understood as arising from the Berry (or Aharonov-Casher) phase accumulated by a quasiparticle/vortex when moving around another quasiparticle/vortex with fractional charge.[4]

As shown in Fig. 1.4, the FQHE is observed also at filling fractions other than $\nu = 1/(2p+1)$. Initially, this was interpreted in terms of a hierarchy scheme [12] which postulates that the fractionally charged quasiparticle excitations of a given FQHE state are able to form a "daughter" Laughlin-type FQHE state. This scenario rests on the observation that there is a correspondence between the original electron system and the system of quasiparticles, since the latter are also charged particles repelling each other via the Coulomb interaction. In this way, one can construct fractional quantum Hall states at all possible odd-denominator filling fractions.

On the other hand, the sequence of quantized Hall states at filling factors $\nu = p/(2p \pm 1)$ (with p integer) is particularly prominent experimentally. While this stability is not easily understood within the hierarchy scheme, it is rather natural in an alternative approach, based on the concept of composite fermions. Within this mean field approximation, the strongly interacting liquid of electrons in the LLL is mapped to a weakly interacting system of composite fermions (CF). Composite fermions (CF) can be viewed as electrons carrying two flux

[4] The Aharonov-Casher phase of a vortex encircling a fluid region equals 2π times the number of fluid particles (here: electrons) enclosed. This phase is fractional due to the fractional charge associated with the enclosed quasiparticle.

quanta.[5] A humorous view of CFs is depicted in Fig. 1.6. Originally, the concept was introduced by Jain in the context of trial wavefunctions [16, 17]. Alternatively, composite fermions can be obtained by means of a Chern-Simons transformation. Writing the electron wavefunction as $\Psi_e(\mathbf{r}_1, \mathbf{r}_2, ..., \mathbf{r}_N)$, where $\mathbf{r}_j$ is the position of the j-th electron, one defines a new wavefunction

$$\Phi(\mathbf{r}_1, \mathbf{r}_2, ..., \mathbf{r}_N) = \left[\prod_{i<j} e^{-2i\theta(\mathbf{r}_i - \mathbf{r}_j)}\right] \Psi_e(\mathbf{r}_1, \mathbf{r}_2, ..., \mathbf{r}_N) \quad , \tag{1.5}$$

where $\theta(\mathbf{r}_i - \mathbf{r}_j)$ is the angle formed by $\mathbf{r}_i - \mathbf{r}_j$ and the $\hat{\mathbf{x}}$-axis. The product prefactor of Ψ_e in the above equation effectively introduces two flux quanta at the position $\mathbf{r}_i$ of each electron. This can be easily seen if one considers the motion of one electron around another on a closed loop which encloses only this specific electron. The resulting change in Φ is a phase factor $\exp(-4\pi i)$ corresponding exactly to the Aharonov-Bohm phase which appears when the trajectory of the electron encloses two flux quanta.

The wavefunction in Eq. (1.5) is also fermionic, since it remains antisymmetric under exchange of two particles. If Ψ_e is a solution to the Schrödinger equation $H_e\Psi_e = E\Psi_e$, then Φ must be a solution of the Schrödinger equation $H\Phi = E\Phi$ with the Hamiltonian

$$H = \frac{1}{2m}\sum_j \left[\mathbf{p}_j + e\mathbf{A}(\mathbf{r}_j) - e\mathbf{a}(\mathbf{r}_j)\right]^2 + \sum_{i<j} v(\mathbf{r}_i - \mathbf{r}_j) \quad , \tag{1.6}$$

where m is the bare electron band mass, v the two-body (Coulomb) interaction potential, $\mathbf{A}$ the vector potential and $\mathbf{a}$ the Chern-Simons vector potential given by

$$\mathbf{a} = \frac{\phi_0}{\pi}\sum_{j=1}^{N} \frac{\hat{\mathbf{z}} \times (\mathbf{r}_i - \mathbf{r}_j)}{|\mathbf{r}_i - \mathbf{r}_j|^2} \quad . \tag{1.7}$$

The factor ϕ_0/π stems from the requirement that the magnetic flux enclosed by a circular trajectory of radius R of one electron around another has to be $2\phi_0$, i.e.

$$\int \mathbf{b}\, dA = \oint \mathbf{a} \cdot d\mathbf{r} = 2\phi_0 \quad . \tag{1.8}$$

The Hamiltonian H can be thought of as being the Hamiltonian for N interacting transformed fermions. The transformed fermions can be interpreted as electrons with two attached flux quanta and are thus called composite fermions.

Due to the resulting Chern-Simons field[6]

$$\mathbf{b} = \nabla \times \mathbf{a} = 2\phi_0 n(\mathbf{r}) \quad , \tag{1.9}$$

the CFs experience an effective magnetic field $B^* = B - b$ which is much weaker than the true magnetic field B,

$$B^* = B - 2\phi_0 n \tag{1.10}$$

[5] In general, any even number $2p$ (with p integer) of flux quanta can be attached to each electron, since any even number of attached flux quanta retains the fermionic nature of the composite particles.

[6] Here, $n(\mathbf{r}) = \sum_j \delta(\mathbf{r} - \mathbf{r}_j)$ is the local particle density.

where ϕ_0 is the flux quantum and n the density of electrons (or, equivalently,[7] CFs).[8] Just as the electrons in the original problem, the CFs form LLs in this reduced field B^*, called CF-LLs. Due to the reduced effective magnetic field, the filling factor of CFs in the CF-LLs,

$$\nu^* = \frac{n\phi_0}{|B^*|} \tag{1.11}$$

is not the same as that of the original electrons in the electron LLs ($\nu = n\phi_0/B$). Instead, the filling factors are related via

$$\nu = \frac{\nu^*}{2\nu^* \pm 1} \quad , \tag{1.12}$$

where the minus sign is for an effective magnetic field B^* antiparallel to B. It is now evident that the principal series of fractional quantum Hall states $\nu = p/(2p\pm1)$ can be interpreted as the integer quantum Hall effect of composite fermions at filling factor $\nu^* = p$.

At $\nu = 1/2$, the Chern-Simons transformation maps the electrons into CFs at vanishing effective magnetic field $B^* = 0$. Naively, the mapping therefore predicts a Fermi-liquid state at this filling factor. Remarkably, there is much experimental and theoretical support for this view, despite the absence of an energy gap. We note for completeness that in addition to the effective magnetic field, composite fermions are also subject to an effective electric field

$$\mathbf{E}^* = \mathbf{E} - \frac{2h}{e^2}\,\mathbf{j} \times \hat{\mathbf{z}} \quad , \tag{1.13}$$

where $\mathbf{E}$ is the physical electric field, $\mathbf{j}$ is the current density and $\hat{\mathbf{z}}$ is the unit vector perpendicular to the plane of the 2DEG.

1.3 High Landau Levels

As the magnetic field becomes smaller and the Fermi energy moves into higher Landau levels, the number of fractional quantum Hall states rapidly decreases. In very-high quality samples, a number of fractional quantum Hall states are observed in the second Landau level (filling factors $2 < \nu < 4$ due to the spin degree of freedom), while no fractional quantum Hall states are observed in higher Landau levels.

The fractional quantum Hall states observed in the second LL include the plateau at filling factor $\nu = 5/2$ (and the particle-hole-symmetry related state at $\nu = 7/2$) which are the only known *even*-denominator states. Fig. 1.7 shows results of a corresponding experiment by Pan *et al.* [18]. A likely scenario for these states is most easily thought of in the context of the composite-fermion

[7] Note that the magnitude of the wavefunction is not altered by the Chern-Simons transformation, Eq. (1.5).

[8] The effective magnetic field is given here for the special case of two flux quanta attached to an electron. In general, as mentioned above, any even number $2p$ (with p integer) of flux quanta could be attached to an electron so that $B^* = B - 2p\phi_0 n$.

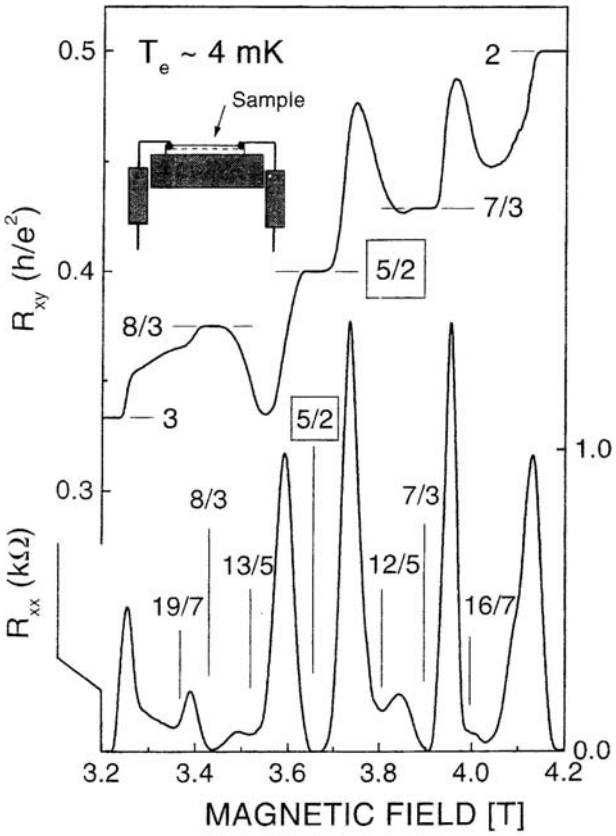

Figure 1.7: The even-denominator state at $\nu = 5/2$ along with the FQHE states at $\nu = 8/3$ and $\nu = 7/3$. Shown are the longitudinal resistance R_{xx} and the Hall resistance R_{xy} at low temperature $T \simeq 4$ mK. The inset shows a schematic sketch of the experimental device. This figure has been taken from Ref. [18].

approach. The Chern-Simons transformation again leads to composite fermions in zero effective magnetic field due to the half-filled valence LL. The composite fermions can then condense into a paired state as in the BCS theory of superconductivity. Due to the flux-charge attachment, the Meissner effect of the resulting superconducting state implies that the state is incompressible and consequently exhibits a Hall plateau. The different nature of the ground states at filling factors $\nu = 1/2$ and $\nu = 5/2$ can be traced back to the different effective interactions in the two cases, originating from the different LL wavefunctions.

The magnetic-field-induced spin polarization of the electron system implies that the pairing occurs in an odd-angular-momentum channel, with p-wave pairing being most favorable [19, 20, 21, 22, 23]. It turns out that the physics of two-dimensional p-wave superconductors is quite rich, with the most important consequence that the excitations of the paired state at filling factor $\nu = 5/2$ are likely to exhibit nonabelian quantum statistics. It has been suggested that other fractional quantum Hall states in the second LL are in fact so-called parafermion states, rather than ordinary Laughlin states [24].

As the Fermi energy moves into even higher LLs, the valence LL wave func-

tions become more and more extended and consequently, the effective interaction more mean-field like. In a seminal paper, Aleiner and Glazman showed [25] that the effective interaction is weak in the sense that the problem of interacting electrons at high Landau level filling factors can still be projected onto a single (valence) Landau level. The weakness of the effective interaction arises due to screening by electrons in the filled Landau levels. Using this effective interaction, Fogler and co-workers [26, 27, 28] as well as Moessner and Chalker [29] showed that the Hartree-Fock (or mean-field) ground states are charge-density-wave (CDW) states whose nature depends on the filling of the valence Landau level. These predictions have later been supported by numerical exact diagonalization studies [30]. It is interesting to note that a charge-density-wave ground state was suggested for the (partially filled) lowest Landau level by Fukuyama, Platzman and Anderson [31] before the discovery of the quantum Hall effect. In the LLL, however, these states are preempted by the Laughlin states due to their lower energies.

In clean 2D electron systems, the instability of the uniform liquid state with respect to the formation of charge density waves occurs for Landau levels $N > 2$. Near half filling of the topmost LL, a compressible, unidirectional stripe phase emerges. In this stripe phase, the electron density in the topmost LL alternates between completely empty (filling factor $\nu = N$) and completely filled (filling factor $\nu = N + 1$) valence LL[9] and one-dimensional stripes of these two kinds arrange with a period of the order of the cyclotron radius R_c. Soon after this theoretical prediction, Eisenstein and collaborators [32] as well as Pan *et al.* [33] observed a striking anisotropy of the resistivity near half filling of higher Landau levels, characteristic of the striped states.

Farther away from half filling of the topmost LL, a bubble phase is predicted theoretically within Hartree-Fock calculations for clean 2D electron systems [27]. In this bubble phase, clusters of minority filling factor with size $\sim R_c$ order regularly on a triangular lattice, submerged in a background of majority filling factor.

To understand the striped phase at finite T and in the presence of disorder, one can rely on an instructive analogy with liquid crystals. Indeed, the striped state shares the symmetries of a smectic liquid crystal [34]. Thus, apart from quantum dynamics at zero T, both systems share the same elastic theory. This implies that the smectic order is lost at any finite temperature in favor of quasi-long-range orientational (nematic) order of stripe segments. Orientational order persists up to a critical temperature, where there is presumably a Kosterlitz-Thouless transition to an isotropic state with only short-range stripe ordering. Similar conclusions can be drawn in the presence of disorder [35].

1.4 This Thesis

In recent years, there have been a number of puzzling experimental discoveries at even higher Landau level filling factors which are the main concern of this

[9] As an example, consider the filling factor $\nu = 9/2$. In this case, there are stripes of the incompressible QHE states $\nu = 4$ and $\nu = 5$ present in the system.

thesis.

Very recently, interesting and unexpected effects have been observed in high-purity samples at low magnetic fields irradiated with microwaves [36, 37]. When an extremely high-purity sample is irradiated with microwaves in the GHz range, its longitudinal resistance develops steep oscillations at very low magnetic fields ($B \sim 0.1$ T), i.e. high filling factors (of the order of $\nu \simeq 50$ and above). For sufficiently high microwave power, the amplitude of these oscillations can grow so large that for certain regions in B, the longitudinal resistance drops to zero within experimental accuracy. The Hall resistance, in contrast, seems to be unaffected by the microwave irradiation and does *not* exhibit plateaus in the regions of zero longitudinal resistance, which would be characteristic of a quantum Hall state. These so-called zero resistance states (ZRS) therefore call for a different theoretical explanation. The microwave-induced oscillations of the resistance and the regions of appearance of ZRS are periodic in $1/B$, reminiscent of the Shubnikov-deHaas oscillations which arise due to the $1/B$-periodic density of states. The period of the new effect in $1/B$, however, is determined by the microwave frequency rather than the Fermi energy.

The first part of this thesis is devoted to the study of microwave-irradiated quantum Hall systems in high Landau levels. In Chapter 2, we give a brief introduction to the experiments on ZRS and their current theoretical description. The central ingredient in their description is a classical *instability* which develops when the microscopic conductivity becomes negative. Very interestingly, a purely classical Drude model with a weakly nonparabolic electron dispersion driven by a microwave field can be shown to yield such zero resistance states. We devote Chapter 3 to this model and, in particular, to the special case of bichromatic irradiation, i.e. irradiation of the 2D electron system with two distinct microwave frequencies. When the detuning between the two frequencies is small, we show that the effect of the weak nonparabolicity of the electron spectrum on the diagonal conductivity of the system is qualitatively the same for monochromatic and bichromatic irradiation. In particular, we demonstrate the emergence of zero resistance states for both cases within our classical model. At strong detuning of the two frequencies, we are able to predict a qualitatively different behavior between monochromatic and bichromatic irradiation. Among other results, we demonstrate a way to parametrically excite the cyclotron mode by bichromatic irradiation. This parametric resonance creates a dc current in the ac-driven system, which should be detectable in experiment. In addition, we find multistable behavior of the diagonal conductivity with respect to the magnetic field, which leads to interesting effects in the transport properties of the system. Finally, we explain how bichromatic irradiation can be used as a tool to demonstrate the physical reality of absolute negative local conductivity which lies at the center of the theoretical explanation of zero resistance states within a microscopic quantum mechanical model. Such an experiment has recently been reported in Ref. [38].

Chapter 4 presents a theory for the recently discovered [39, 40] magnetooscillations and the suppression of the Shubnikov-deHaas oscillations in the intra-Landau-level regime, i.e. for microwave frequencies ω smaller than the cyclotron frequency ω_c. We formulate a microscopic model which mimics the effect of a

smooth random disorder potential by the introduction of a periodic modulation potential and calculate the conductivity of the system under microwave irradiation. Previous work shows that the results obtained in this way are parametrically identical to those for models taking into account disorder on a microscopic level when one identifies the broadening of the Landau levels by the additional modulation potential with disorder broadening. We are able to explain why no ZRS are observed in the intra-LL-regime. In addition, we reproduce the sign of the photoconductvity, its magnetic field and frequency dependence as well as its filling factor dependence in excellent qualitative agreement with experiment and discuss the polarization dependence of our results.

The application of an in-plane magnetic field to a high-mobility 2DEG under microwave irradiation showing ZRS in a perpendicular magnetic field has been demonstrated experimentally [41] to induce a pronounced suppression or even destruction of the ZRS for sufficiently strong parallel components of the magnetic field. This experimental result will be considered in Chapter 5. We calculate the effect of a tilted magnetic field within a kinetic approach for spin-split Landau bands and estimate the relevance of the Zeeman splitting for the suppression of ZRS.

The second part of this thesis is devoted to the physics of drag phenomena in bilayer quantum Hall systems. When a current flows in one layer of a bilayer system, electron-electron interactions between the layers can lead to a momentum transfer to the other layer, and thus to the emergence of a current. If the layers are in close proximity, Coulomb electron-electron interactions constitute the dominant channel for momentum exchange between the layers. At larger interlayer separations, however, other mechanisms of momentum transfer, like, e.g., phonon-mediated electron-electron interactions, might become relevant. In contrast to Coulomb drag, which has been studied extensively, the effect of phonon drag in a finite magnetic field remains to be understood. In this thesis, we present a theory for phonon drag in bilayer systems at weak magnetic fields, i.e. in high Landau levels.

Chapter 6 provides an introduction to the physics of drag phenomena by reviewing the current state of experiment and theory. The chapter also gives a brief introduction to the linear response formalism for the calculation of the drag conductivity.

Chapter 7 is devoted to our microscopic theory of phonon drag in high Landau levels. For Coulomb drag, the interlayer interaction is suppressed at large momentum transfers by a factor $\exp(-qd)$, so that the Coulomb drag contribution to the drag conductivity is governed by small momenta $q < 1/d$. This introduces a natural cutoff on the momentum exchange between the layers. Such a cutoff is absent in the case of phonon drag. We therefore need to extend the linear response formalism to finite momentum transfers. This is done in detail in Chapter 7. We also derive the phonon-mediated interlayer interaction in this chapter. We then present analytical results for the phonon drag conductivity in the low temperature regime. To further illustrate the behavior of phonon drag, we also present numerical calculations of the phonon drag resistivity for realistic parameter sets. Finally, we close in Chapter 8 by summarizing our main results and giving an outlook to promising avenues for future research.